DESIGN STUDY OF THE MONIKA ORC-TURBINE AND COMPARISON WITH EXPERIMENTAL RESULTS

H.-J. Wiemer[1]*, C.L. Niño Avella[1], T. Schulenberg[1]

[1] Karlsruhe Institute of Technology, Institute of thermal energy and safety, Karlsruhe, BW, Germany

* *Corresponding Author: wiemer@kit.edu*

Abstract. This study presents the development, verification, and validation of a MATLAB code for conducting a mean-line analysis of a four-stage Organic Rankine Cycle (ORC) turbine with a power output of around 100 kW, operated with supercritical propane at the Karlsruhe Institute of Technology (KIT). Typically, a mean-line analysis is performed for an envisaged design point during the initial phase of turbomachinery design. In this study, it is used to analyse the performance and efficiency of a turbine at different operating conditions. Accuracy checks were carried out to validate the applied loss correlations. The ORC turbine was installed in the MONIKA test facility, a modular geothermal power plant, which was tested here using a simulated heat source instead. Propane at a design pressure of 5.5 MPa and a temperature of 390 K, undergoes expansion to an outlet pressure of 1.1 MPa. During the tests, however, the test conditions deviated significantly from the original design, and nitrogen leakage into the propane cycle could not be prevented from the turbine sealing system. The mean-line analysis confirms that the developed code can still predict the ORC turbine's performance and attributes with reasonable accuracy. Additionally, the software can analyse the impact of different design alterations on the thermodynamic properties of the fluid at the inlet and outlet, as well as on the performance of the turbine.

Keywords. Supercritical-Organic-Rankine-Cycle, Turbine-Design, Mean-line-analysis.

Nomenclature (if relevant)

An	Area of cross section $[m^2]$
At	Throat area of vanes $[m^2]$
ca	Vane/Blade chord length $[m]$
dq	Specific energy losses $[J/kg]$
F	Fraction of aperture
h	Specific enthalpy (J/kg)
Hb	Blade height [m]
s	Specific entropy [J/kgK]
tvp	Throat of a vane passage [m]
T	Temperature (K)
M	Mass flow [kg/s]
Mv	Vane mass flow [kg/s]
Ml	Leakage mass flow [kg/s]
P	Pressure (kPa)
PR	Pressure ratio
Pturb	Turbine power [W]
PV	Ventilation power [w]
qFE	Spec. filling/emptying losses [J/kg]
qV	Spec. energy by ventilation [J/kg]
R	Radius [m]
U	Blade velocity [m/s]
V	Abs. Velocity [m/s]
W	Relative Velocity [m/s]
zl	Number of labyrinth tips

Special characters

α	Outlet angle vanes [*rad*]
β	Outlet angle blades [*rad*]
ε	Deflection angle [*rad*]
ζ	Soderberg loss coefficient [-]
ρ	Density [kg/m^3]
ω	Angular velocity $[rad/s]$
Ω	Aperture angle $[rad]$
η_{turb}	Turbine efficiency [-]

Subscripts

ax	Axial
u	Circumferential
n	Cross section number

1 Introduction

A usual technology for thermal energy sources with a temperature in the range of 100°C to 260°C is the Organic Rankine Cycle (ORC). These sources include geothermal reservoirs and industrial waste heat. In this cycle, organic liquids are used as working fluids instead of steam to extract electrical energy from low-temperature heat sources more efficiently.

The globally installed capacity of ORCs in renewable energy and waste heat plants has grown rapidly in recent years. It is estimated that there is now about 2000 MW of installed capacity in plants using ORC cycles [1].

The focus of this paper is on the turbine of the MONIKA (Modular Low Temperature Cycle Karlsruhe) project, a facility of the Institute for Thermal Energy and Safety (ITES) at the Karlsruhe Institute of Technology (KIT). The MONIKA plant consists of an ORC cycle with supercritical live steam parameters and propane as working fluid. As MONIKA is an experimental facility, an artificial heat source is producing hot water, which has been adjusted to a temperature of 150°C for the experiments.

The work focuses on the study of MONIKA's axial 4-stage impulse turbine, which is one of the main components of the system along with the pump, evaporator and condenser, as it is responsible for converting the enthalpy of the fluid into mechanical energy through expansion.

In order to analyse the behaviour of the MONIKA ORC turbine, this work deals with the calculation of the stage parameters based on a mean line analysis in steady-state operation. The results obtained are compared with the characteristics provided by the manufacturer [3] and with experimental data of Perez [2], which showed the behaviour of the turbine under different operating conditions.

The aim of this study was to develop a MATLAB code utilizing balance equations and loss correlations for axial turbines. The code can predict the thermodynamic properties, power, and efficiency of a turbine-based a given geometry of the turbine and its inlet/outlet conditions. The results are validated using measured data. More details can be found in [4].

The essential geometric features, such as cross sections, blade exit angles, and labyrinths, are taken from CAD data provided by the turbine manufacturer [3].

With the developed code, we are able to predict the behaviour of the turbine under different operating conditions, varying characteristics such as pressure or temperature at the inlet and the pressure at the outlet of the turbine. In addition, we can examine the influence of impurities of the working fluid on the turbine parameters.

2 Materials and Methods

The After compression, a supercritical Rankine cycle heats the working fluid to pressures and temperatures above its critical point. Unlike superheated, subcritical cycles, this cycle facilitates a smooth transition from subcooled liquid to superheated vapor above the critical point during the heat exchange phase. Evaporation occurs gradually, and all properties change continuously during the heating process. In organic Rankine cycles, working fluids have lower critical pressures and temperatures than water. This makes it easier for them to reach supercritical conditions, resulting in better heating performance.

This is especially advantageous when the temperature of the heat source is limited. By selecting the appropriate working fluid, one can find a heating curve that matches approximately the cool-down curve of the heat source. This reduces the logarithmic mean temperature difference and, consequently, exergy losses [5].

2.1 The MoNiKa facility

The MONIKA power plant is a facility located in the Karlsruhe Institute of Technology, Campus Nord. It consists of a generic steam cycle like a geothermal power plant. The cycle is modular and offers unique opportunities for the study of low-temperature electricity generation.

The different components of the facility are presented in Figure 1. The red line represents the cycle when the turbine is running under normal operation conditions, while the dashed line indicates the turbine bypass. The major components of the power plant are the turbine, condenser, propane tank, heat exchanger and pumps.

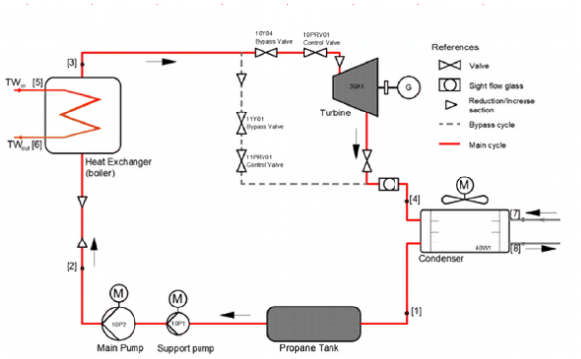

Figure 1: MONIKA POWER PLANT

2.2 *ORC-Turbine*

The 4-stage axial impulse turbine GT 120 – 4 (Fig. 2) manufactured by M+M Turbinen-Technik GmbH, is positioned between the heat exchanger and the condenser. The turbine table, which contains the gearbox and the 4-pole synchronous generator, is installed on vibration dampers in a 10 feet sea container. The turbine maintains a constant blade cross-section while running at a nominal speed of 9960 rpm. A unique feature of this turbine is the partial admission of the guide vanes for all stages (Figure 3). This design differs from the usual standard, where only the first row of guide vanes is partially admitted. The turbine operates at an inlet pressure of 5.5 MPa and an inlet temperature of 117°C according to the design data. It is expected to produce a power output of 139 kW.

Table 1: Design data of the ORC Turbine [3]

GT 120 – 4	
Propane mass flow	2.9 kg/s
Rotor speed	9960 rpm
Turbine inlet pressure (abs)	5.5 MPa
Turbine outlet pressure (abs)	1.1 MPa
Turbine inlet temperature	117 °C (390 K)
Power (Calculated)	139 kW

Figure 2: Monika ORC-Turbine and gearbox without isolation.

For operation, nitrogen is used as a sealing gas, which prevents propane leakage through the casing to the environment. Unfortunately, there was a residual amount of N_2 inside the working fluid during operation, which has to be taken into account in the validation analyses.

As shown in Figure 3, there are three labyrinth tips each inside the vane discs 2 to 4, which produce a leakage mass flow to be taken into account.

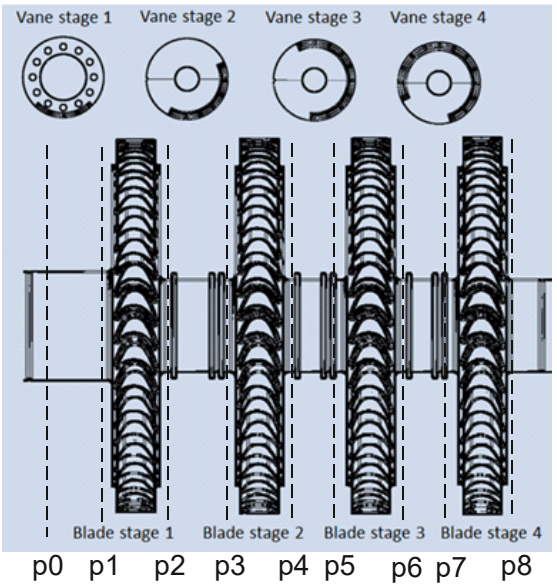

Figure 3: Rotor design and open vane passages

Equation 1 shows how the outlet angle α of the vane can be determined from the throat area At and the cross-section area An of a vane. Here, tvp is the throat of a vane passage, hb the vane height, ovp the number of open vane passages, R_e the outer radius of the vane, R_i the inner radius of the vane and Ω the aperture angle of the vane cross section.

$$\sin(\alpha) = \frac{At}{An} = \frac{2*tvp*hb*ovp}{\Omega({R_e}^2-{R_i}^2)} \qquad (1)$$

The blade outlet angle b is measured at the mean radius by extending the pressure side of the blade.

The chord length "ca" is used instead of the axial width, as shown in Figure 4 for vanes on the left and blades on the right-hand side. This approach conservatively increases the losses using the Soderberg correlations [9].

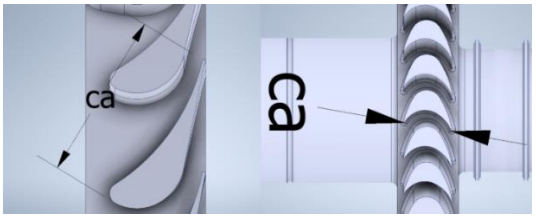

Figure 4: Chord length of vanes and blades

2.3 Measured experimental data

The facility has pressure and temperature sensors at the turbine inlet and outlet, as indicted in Fig 1. The mass flow sensor is situated behind the main pump. These sensors continuously transmit data to the control unit, which are averaged for the analysis of each run. To ensure consistent results, only steady-state conditions are selected, when the bypass valve is entirely closed. These measurements were extracted from a previous work of Perez [2], which details the pressure, temperature, mass flow of the fluid, and power output under varying conditions, Table 2. The measurements were taken on the first day of the study, 8 November 2021, and on the second day, 9 November 2021.

The turbine outlet pressure is observed to range from 1035 to 1128 kPa, with the former value corresponding to smaller mass flows and the latter to larger mass flows.

Table 2: Measured data from test runs [2]

Day/ Run	Mass Flow [kg/s]	Valve Inlet Temp. [K] (2p)	Valve Inlet Pressure [kPa] (2p)	Turb. Power [kW]
1/4.	2.2	381.3	5189.7	96.0
1/6.	1.9	383.1	5190.4	83.7
2/3.	2.6	383.6	5627.1	102.2
2/4.	2.6	382.5	5499.3	102.6
2/5.	2.6	382.1	5427.7	103.4
2/6.	2.6	380.8	5295.3	103.1
2/7.	2.6	379.9	5196.9	103.8
2/8.	2.6	379.2	5131.0	103.6
2/9.	2.7	379.9	5219.9	104.4

2.4 Reference data base Refprop

The thermodynamic properties of pure propane and propane-nitrogen mixtures have been determined with REFPROP 9.1 [7]. REFPROP uses the Kunz and Wagner model for hydrocarbon mixtures [8], to calculate the thermodynamic properties of the propane-nitrogen mixture. From the experimental data, we determined the nitrogen content using the measured pressure and temperature at the turbine outlet to 1.6 %mass.

2.5 Turbine inlet conditions

The stagnation conditions at turbine inlet are determined from the measured data upstream the turbine inlet valves (marked as '2p' in Fig. 1). Under supercritical conditions, the measured pressure and temperature determine the enthalpy h, entropy s and density ρ there. Knowing the heat losses h1loss between these two points, the enthalpy at turbine inlet (1p) is determined then as:

$$h_{1p} = h_{2p} - h_{1loss} \tag{2}$$

With the measured pressure in (1p), the calculated enthalpy h_{1p} determines all other mixture properties there. Finally, the static pressure at turbine inlet (0p) is determined from these data at (1p) assuming an adiabatic acceleration of an incompressible flow.

2.6 Turbine mean line analysis

A mean line analysis is considering a 3D flow through a turbine, which is averaged in radial and circumferential direction as well as in time. In this particular case of an axial turbine, the radial velocity component is even considered to be zero [9]. Pressures, enthalpies and velocities are determined only for each axial cross section at the inlets and outlets of turbine vanes and blades, indicated as p0 to p8 in Fig. 3 and numbered by n = 0 to 8, while the details of flow inside these stages are taken into account by empirical loss correlations. The balance equations for these axial cross sections are: The conservation of mass, Eq. (3), Euler's equation (4) (shown exemplarily for blade 1), and conservation of energy, Eq. (5). Here, the mass flow is denoted by M, the axial cross-section by An, the speed in the absolute system by V and in the rotating system by W, the rotor speed by U, the specific turbine work by dA, and the energy losses by dq [6].

$$M = \rho A n V_{ax} = constant \tag{3}$$

$$dA = \frac{{U_1}^2 - {U_2}^2}{2} + \frac{{V_1}^2 - {V_2}^2}{2} - \frac{{W_1}^2 - {W_2}^2}{2} \tag{4}$$

$$d\left(h + \frac{1}{2}V^2\right) = dA + dq \tag{5}$$

Unlike conventional methods, where the enthalpies in these cross sections are taken as input to determine the required flow angles of vanes and blades, the outlet flow angles are taken from the given design, as described in section 2.2. The balance equations are solved iteratively, starting from an initial guess of the pressure distribution, such that mass flows, velocities and enthalpies can be determined for each stage. The pressure distribution is iterated then until the mass flow of each stage becomes identical. This uniform

mass flow, as well as the predicted turbine power, can be compared then with the measured ones for validation. The method is outlined by Traupel [6]. The energy losses in Eq. (5) are determined by a loss correlation of Soderberg as recommended by Dixon [10].

It's important to note that the empirical correlations used to determine losses within the turbine were derived only for gases or steam. If the fluid entering the turbine has a high liquid fraction, bubbles will form in the first stage of the blades, resulting in cavitation similar to that of a pump. As such, the fluid is beyond the scope of the correlations that are to be used. Only vapor qualities greater than 0.8 are considered to be correct.

2.7 Initial pressure distribution

To enable comparison of the mean line analysis with measure data, the inlet and outlet pressures as given in Tab. 3 are taken as boundary conditions. They are used also to determine the initial pressure distribution at different cross sections for the iterative procedure.

This initial guess of the pressure distribution is assuming the same pressure ratio for each stage as the total pressure ratio PR of the entire turbine. With $P_0 =$ inlet pressure and $P_8 =$ outlet pressure, we get:

$$PR = \frac{P_0}{P_8} \tag{6}$$

Consequently, we obtain the pressure at each vane outlet as

$$P_{2m-1} = \frac{P_{2m-2}}{PR^{1/4}} \tag{7}$$

with m=1 to 4 as the stage number.

In case of an ideal impulse turbine, like in our case, an initial guess of the pressure at blade outlets is:

$$P_{2m} = P_{2m-1} \tag{8}$$

2.8 Velocity of the blades

In a mean line analysis, the circumferential component Uu of the rotor velocity equals the mean radius Rm times the angular velocity ω. In the particular case of the MONIKA turbine, the mean radius is constant and consequently the blade velocity. Therefore, we get for each cross-section n =1 to 8

$$\omega = 2\pi f \tag{9}$$

$$U_{ax,n} = 0 \tag{10}$$

$$U_{u,n} = R_{m,n}\omega \tag{11}$$

In Eq. (9), f is the rotor frequency.

2.9 Calculation for a vane row

The index n at vane outlets is 1, 3, 5, or 7. The following procedure is repeated for each vane outlet.

The first step is to find the isentropic enthalpy $h_{s,n}$ by using the entropy s_{n-1} from the previous step and the prescribed pressure P_n for this step. If n = 1, the entropy used corresponds to the inlet entropy s_0 of the turbine.

$$h_{s,n} = h(P_n, s_{n-1}) \tag{12}$$

To determine the energy losses, we used the Soderberg loss correlation [10] to derive the loss coefficient ζ_n'. In Eq. (13), ε_n is representing the blade deflection angle that results from the difference between the inlet angle α_{n-1} and the outlet angle α_n. With the loss coefficient given by Eq. (13), the chord length ca_n and the blade height hb_n, we can calculate the overall loss of each blade row ζ_n as shown in Eq. (15).

$$\zeta_n' = 0.04 + 0.06 * \left(\frac{\varepsilon_n}{100}\right)^2 \tag{13}$$

$$\varepsilon_n = \alpha_n - \alpha_{n-1} \tag{14}$$

$$\zeta_n = (1 + \zeta_n') * \left(0.993 + 0.021 * \frac{ca_n}{hb_n}\right) - 1 \tag{15}$$

The vane efficiency η be expressed as function of the losses, as:

$$\eta_n = 1 - \zeta_n \tag{16}$$

With the vane efficiency and the isotropic enthalpy, we calculate the actual enthalpy at vane outlet as:

$$h_n = h_{n-1} - \eta_n(h_{n-1} - h_{s,n}) \tag{17}$$

Using REFPROP, we can determine the following properties of the fluid from the given enthalpy and pressure in each cross-section n.

$$s_n = s(h_n, P_n)$$

$$\rho_n = \rho(h_n, P_n)$$

$$T_n = T(h_n, P_n)$$

From the energy balance, we can express the change in enthalpy as a change in kinetic energy using Eq. (18). Here, V represents the absolute velocity at the vane inlet *(n-1)* and outlet *(n)*.

$$\frac{{V_n}^2}{2} - \frac{{V_{n-1}}^2}{2} = h_{n-1} - h_n \tag{18}$$

The mass flow Mv_n through the vane channels correlates with the fluid velocity and density, as:

$$V_n = \frac{Mv_n}{\rho_n An_n sin\alpha_n} \tag{19}$$

$$V_{n-1} = \frac{Mv_n}{\rho_{n-1} An_{n-1} sin\alpha_{n-1}}$$

Since the mass flow at the inlet and outlet of the vane is constant, we can combine Eqs. (18) and (19) to yield:

$$Mv_n = \sqrt{2 * (h_{n-1} - h_n)} * \sqrt{\left(\frac{1}{(\rho_n An_n sin\alpha_n)^2} - \frac{1}{(\rho_{n-1} An_{n-1} sin\alpha_{n-1})^2}\right)} \tag{20}$$

After calculating the mass flow through the vanes, we determine the velocity component V_{ax} and V_u in the absolute system as:

$$V_{ax,n} = \frac{Mv_n}{\rho_n An_n} and\ V_{u,n} = \frac{V_{ax,n}}{tan\ \alpha_n} \tag{21}$$

$$|V_n| = \sqrt{{V_{ax,n}}^2 + {V_{u,n}}^2} \tag{22}$$

As previously stated, the mass flow rate *Mv* only relates to the flow through the vane passages. For a more precise calculation, the leakage mass flow rate through the labyrinth tips *Ml* must be taken into account as well. This is affected by the labyrinth's geometry, fluid density, number of tips *z1*, and pressure ratio upstream and downstream the tips [11]. With the labyrinth's tip diameter *(DL)* and the distance *(HL)* between the tips, we can determine the leakage mass flow as:

$$Ml1_n = 0.8 * \pi * DL * HL * \sqrt{\rho_{n-1} P_{n-1}} \tag{23}$$

$$Ml_n = ML1_n * \sqrt{\frac{1 - \left(\frac{P_n}{P_{n-1}}\right)^2}{z1 + \ln\left(\frac{P_{n-1}}{P_n}\right)}} \tag{24}$$

Finally, the mass flow *M* through the stage equals the total vane mass flow as:

$$M_n = Mv_n + Ml_n \tag{25}$$

This mass flow is taken as well for the blade row of each stage, such that

$$M_{n+1} = M_n \tag{26}$$

2.10 Calculation for a blade row

Once the stage mass flow has been determined, we can continue with the blade outlet at cross sections n=2, 4, 6, 8. The velocity at blade inlet equals the vector sum

$$\vec{W}_{n-1} = \vec{V}_{n-1} - \vec{U}_{n-1} \tag{27}$$

which defines the inlet flow angle β_{n-1}:

$$\beta_{n-1} = \text{atan}\left(\frac{W_{ax,n-1}}{W_{u,n-1}}\right) \tag{28}$$

The blade outlet angle β_n is taken from the CAD data as described in section 2.2. Thus, we get the blade outlet velocity *W* in the rotating system as

$$W_{ax,n} = \frac{M_n}{\rho_n An_{n-1}} and\ W_{u,n} = \frac{W_{ax,n}}{tan\ \beta_n} \tag{29}$$

Here, however, the density ρ_n at blade outlet must be iterated. As an initial guess, we assume that the density remains constant.

The density is a function of enthalpy and pressure at blade outlet. The blade outlet enthalpy can be determined by the energy equation (5), as will be described next.

The Soderberg correlation is once again taken to calculate the internal blade losses. It should be noted that the expression used for the blades differs slightly from that of the vanes [10]:

$$\zeta_n{}' = 0.04 + 0.06 * \left(\frac{\varepsilon_n}{100}\right)^2 \tag{30}$$

The blade deflection angle ε_n is determined by the inlet and outlet angles β_{n-1} and β_n of the blades as:

$$\varepsilon_n = \beta_n - \beta_{n-1} \tag{31}$$

With the Soderberg's loss coefficient,

$$\zeta_n = (1 + \zeta_n{}') * \left(0.975 + 0.075 * \frac{ca_n}{hb_n}\right) - 1 \tag{32}$$

we determine the blade efficiency as:

$$\eta_n = 1 - \zeta_n \tag{33}$$

The energy balance is giving us the enthalpy at blade outlet as:

$$h_n = h_{n-1} + \tfrac{1}{2}(|W_{n-1}|^2 - |W_n|^2 - |U_{n-1}|^2 + |U_n|^2) \tag{34}$$

Together with Eq. (17), we can use this energy balance to determine the isentropic enthalpy $h_{s,n}$ at blade outlet as:

$$h_{s,n} = h_{n-1} - \left(\frac{|W_n|^2}{2\eta_n}\right) + \frac{1}{2}(|W_{n-1}|^2 - |U_{n-1}|^2 + |U_n|^2) \tag{35}$$

Now, the pressure at blade outlet can be calculated with REFPROP from the entropy at blade inlet and the isentropic enthalpy at blade outlet as $P_n = P(h_{s,n}, s_{n-1})$. For turbines with partially open vane channels, known as partial admission, the blades are running temporarily through stagnant regions, causing ventilation losses. According to Traupel [6], the ventilation power, PV, can be predicted as:

$$PV_n = \pi C_n (1 - F_{n-1}) \rho_n 2R_{m,n} hb * {U_{u,n}}^3 \tag{36}$$

with the aperture fraction $F = \Omega/(2\pi)$. The ventilation coefficient C_n varies depends on the structural arrangement and on the direction of turbine rotation. For the MONIKA turbine, the expression is given in [5] for wreath wrapped, forward directed flow as:

$$C_n = 0.0095 + 0.55 * \left(0.125 + \frac{hb_n}{2R_m}\right)^2 \tag{37}$$

The ventilation power and mass flow rate determine the ventilation losses qV_n as:

$$qV_n = \frac{PV_n}{M_n} \tag{38}$$

An additional effect of partial admission results near the active zone due to the inflow from the admission into the blade section (filling) and outflow from the rotor out of the blade section (emptying). These losses are directly proportional to the blade's circumferential velocity $U_{u,n}$ [12].

$$qFE_n = \frac{0.21 ca_n U_{u,n} \sqrt{h_{n-1} - h_{s,n}}}{F_{n-1} 2R_{m,n}} \tag{39}$$

Including these ventilation losses, filling losses, and emptying losses, we get the enthalpy at blade outlet as:

$$h'_n = h_n + qV_n + qFE_n \tag{40}$$

This corrected blade outlet enthalpy and the blade outlet pressure allow now to iterate the outlet density as $\rho_n = \rho(h'_n, P_n)$. Having determined the velocity W_n in the rotating system, we get the velocity V_n in the absolute system at the inlet of the next vane as:

$$\vec{V}_n = \vec{W}_n + \vec{U}_n \tag{41}$$

2.11 Convergence of the method

This method is predicting so far, a different mass flow for each turbine stage. Therefore, the pressures at vane outlets with n=*1, 3, 5* must be iterated until the mass flows through all turbine stages become identical. We know from Stodola's law that the mass flow through a turbine stage is approximately proportional to the pressure at its inlet. Thus, the pressure P_1 is proportional to the mass flow through the second stage, P_3 is proportional to the mass flow through the third stage, etc. The relative mass flow error of the second and higher stage, compared with the inlet mass flow M_0, is:

$$dM_n = \frac{M_n}{M_0} - 1 \tag{42}$$

With this mass flow error, a pressure correction dP_n is calculated for *n=1, 3, 5* as:

$$dP_n = -P_n * dM_{n+2} \quad (43)$$

For each iteration, the new pressure distribution $P_{n,new}$ is then:

$$P_{n,new} = P_n + dP_n * FR \quad (44)$$

An under-relaxation factor *FR* has been included here to avoid negative pressures during iterations. With the new pressure distribution, the mean line analysis described above is iterated until the mass flow error becomes negligible.

After all variables have converged, the turbine power P_{turb}, the turbine efficiency η_{turb} and turbine mass flow can be predicted.

With *M* as the turbine mass flow after convergence, we get the turbine power as:

$$Pturb = M(h_0 - h_8) \quad (45)$$

With REFPROP, we determine the isentropic enthalpy hs,8 at turbine outlet as: $h_{s,8} = h(P_8, s_0)$ From this, we get the turbine efficiency as:

$$\eta_{turb} = \frac{h_0 - h_8}{h_0 - h_{s,8}} \quad (46)$$

2.12 Verification under design conditions

These equations were programmed in a MATLAB code, which was verified by comparison with the design data, Tab. 1. Ideal conditions were assumed, with pure propane as the working fluid. An under-relaxation factor *FR=0.5* has been chosen to reach best conversion. According to the design point, the inlet conditions were supercritical and the outlet pressure was set at 1100 kPa for this calculation.

Table 3: Results and deviation from design data

Item	Unit	Design	Calc	Err
Turbine Power	kW	139	137.	1%
Turbine effic.	%	-	78	-
Mass flow	kg/s	2.9	2.84	2%

Table 3 shows good agreement with the design data. The error is in the order of 1 to 2 %. We can conclude that the loss correlations, i.e., the blade and vane efficiency calculated through the Soderberg correlation, ventilation losses, filling and emptying losses, and labyrinth losses, that account for bypass mass flow via the seals, are appropriate for this application. More convincing, however, will be a comparison with measured data, as will be described next.

3 RESULTS AND DISCUSSION

The method described in Chapter 2.6 was used to determine the properties at the turbine inlet, using the data listed in Table 2 as input data. The achieved results are presented in Table 4. It is important to note that these results reflect the average of steady-state measurements taken under conditions with the bypass valve being completely closed. The nitrogen content in the propane was 1.6 %mass. The critical pressure in this case is 4791.4 kPa and the critical temperature is 371.34 K.

According to the results obtained, the fluid that entered the turbine was sometimes subcritical, but always superheated.

Table 4: Inlet properties of the turbine

Run		Enthalpy [kJ/kg]	Entropy [kJ/kgK]	Pressure [kPa]	Temp. [K]
Day 1	4th	623.159	2.322	4288.47	369.22
	6th	634.859	2.364	3876.54	365.07
Day 2	3rd	606.421	2.268	4793.05	374.31
	4th	608.484	2.273	4798.66	374.60
	5th	611.477	2.281	4811.32	375.10
	6th	612.920	2.285	4804.55	375.17
	7th	615.636	2.292	4825.04	375.77
	8th	615.677	2.292	4822.86	375.74
	9th	612.825	2.283	4909.43	376.53

Following the procedure described in Chapter 2, the properties for each turbine cross section were calculated and iterated. The measured pressures at the turbine inlet and outlet were used to determine the initial pressure distribution for each case. A relaxation factor of FR=0.5 was assumed for this analysis. Fig. 5 show the enthalpy entropy (h-s)-diagram of the predicted turbine expansion. The critical point is at the left end of the saturation line. These results are typical for an impulse turbine with almost constant pressure across the blades.

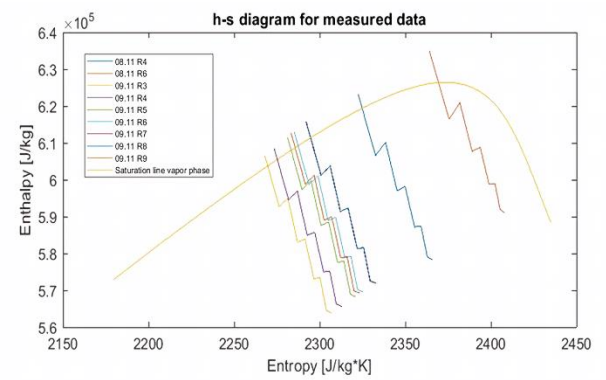

Figure 5: h-s Diagram for measured data

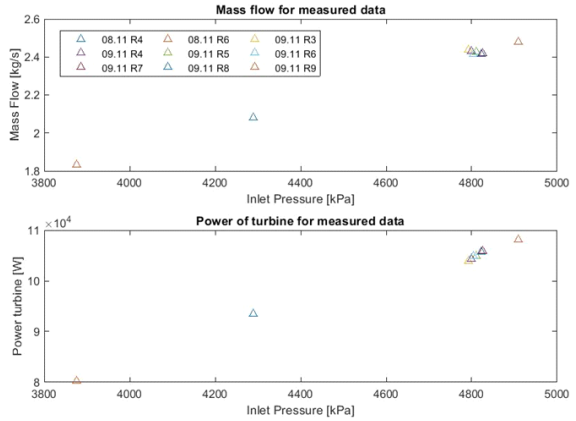

Figure 6: Mass flow and power output calculated with measured data

The fluid's inlet pressure and temperature significantly impact the power generated by the turbine. On days, when the fluid does not reach the supercritical conditions at the turbine inlet, the generated power is lower. Although these values are lower than those at design conditions, the turbine's overall efficiency is not significantly affected. This is because the reduction in generated power is directly related to the reduction in mass flow, and the enthalpy drop in the various stages of the turbine is similar in all cases.

Table 5: Mass flow, power output, efficiency and the error in regard to Measured values

		Calculated			Error	
	Run	M [kg/s]	Power [kW]	Eff.	M	Power
Day 1	4th	2.08	93.420	0.77	5%	3%
	6th	1.83	80.174	0.77	4%	4%
Day 2	3rd	2.43	103.812	0.78	6%	-2%
	4th	2.43	104.228	0.78	7%	-2%
	5th	2.42	104.922	0.78	7%	-1%
	6th	2.41	104.802	0.78	7%	-2%
	7th	2.41	105.819	0.78	7%	-2%
	8th	2.41	105.698	0.78	7%	-2%
	9th	2.47	108.138	0.78	8%	-4%

Table 5 shows the predicted turbine performance in comparison with measured results. A positive sign of the error indicates that a higher value was measured. The predicted power agrees reasonably well with the measured ones, whereas the mass flow turned out to be underpredicted by 4 to 8 %. This might be caused by slight modifications in the vane outlet angles, either due to our analysis or caused by manufacturing, which can heavily impact the turbine mass flow. Additionally, discrepancies in calculating the bypass flow through the seals could further contribute to the observed deviations.

In summary, it can be concluded that the difference between the implemented calculation method and measured data for generated power ranges from -4% to 4%, and for mass flow rate it ranges from 4% to 8%. We considered this result to be accurate enough for validation and the method can be used to predict the turbine performance under different operating conditions.

4 SENSITIVITY STUDY

The benefit of this mean line analysis shall be illustrated with an exemplary result of our sensitivity analyses, for which the turbine inlet temperature was kept constant at the design temperature of 390 K, while the pressure at turbine inlet was decreased in steps of 162 kPa, between P_{max} = 5500 kPa, the design pressure, decreasing to P_{min} = 3877 kPa, the minimum pressure recorded on day 1. The outlet pressure was fixed at 1000 kPa for all cases. The fluid was assumed to be pure propane, which has a critical pressure of 4251 kPa and a critical temperature of 369.8 K

Figure 7 depicts that the enthalpy drop in the first turbine stage will increase with decreasing turbine inlet pressure, and the fluid will be still be superheated at turbine outlet if the inlet pressure is less than 5200 kPa. Accordingly, power and mass flow of the turbine are decreasing with decreasing turbine inlet pressure. Such studies can be important to optimize an ORC power plant for given heat source conditions.

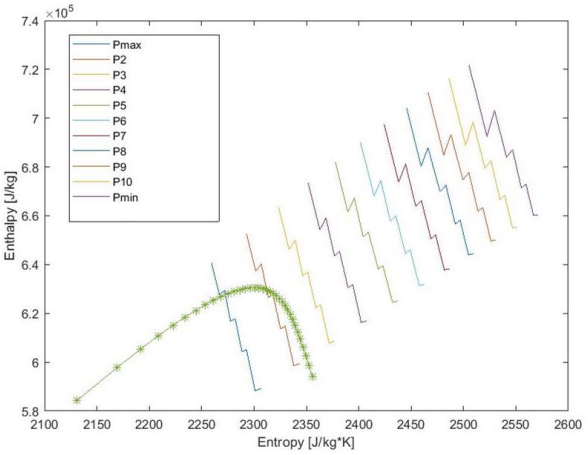

Figure 7: h-s diagram for varying turbine inlet pressure

5 CONCLUSION

A mean line analysis is a powerful tool not only to design a turbine, but also to study its behaviour under varying operating conditions. The method described here can be applied to any given turbine even in case that the working fluid is contaminated with non-condensable gases. The loss correlations, which we implemented here, are typical for multistage, axial impulse turbines with partial admission in the first stage or even, like in the case discussed here, in all turbine stages. The good agreement with measured data is encouraging us to use these loss correlations for future design of ORC turbines for low temperature applications.

References

[1] P. Colonna, E. Casati, C. Trapp, T. Mathijssen, J. Larjola, T. Turunen-Saaresti and A. Uusitalo, "Organic Rankine Cycle Power Systems: From the Concept to Current Technology, Application, and an Outlook to the Future," vol. 137, no. 10, pp. 100801-1-100801-19, 2015.

[2] J. M. Perez, "Experimental examination of the MONIKA-ORC-Turbine and comparison of the results with thermodynamical calculation," Master Thesis, ITES, Karlsruhe Institut für Technologie, Karlsruhe, 2022.

[3] M.TURBINE-TECHNIK, "Turbinenanlage Propan- expander: Project 1 15 3514 0 2018".

[4] C.L. Niño Avella, Design study of the MONIKA-ORC-Turbine and comparison with experimental results, Master Thesis, ITES, Karlsruhe Institut für Technologie, Karlsruhe, 2023, https://doi.org/10.5445/IR/1000170045

[5] E. Macchi, M. Astolfi, Organic Rankine Cycle (ORC) Power Systems Technologies and Applications ISBN: 978-0-08-100510-1, Elsevier, 2017.

[6] W. Traupel, Thermische Turbomaschinen Thermo- dynamisch-strömungstechnische Berechnung, ISBN : 978-3-642-62102-4, Verlag Berlin Heidelberg: Springer, 2001.

[7] Eric Lemmon, Ian H. Bell, Marcia L. Huber, and Mark O. McLinden. NIST Standard Reference Database 23: Reference Fluid Thermodynamic and Transport Properties-REFPROP, Version 9.1, National Institute of Standards and Technology, 2018. Available https://www.nist.gov/srd/refprop. [Accessed 12 January 2023]

[8] W. Wagner, O. Kunz, R. Klimeck and M. Jaeschke, Wide-Range Equation of State for Natural Gases and Other Mixtures, ISBN 978-3-18-355706-6, Düsseldorf: GERG, 2007.

[9] E. Dick, Fundamentals of Turbomachines ISBN 978-94-017-9627-9, Dordrecht: Springer, 2015

[10] S. L. Dixon, Fluid Mechanics, Thermodynamics of Turbomachinery ISBN 0 7506 7059 2, Oxford, UK: Butterworth-Heinemann, 1998.

[11] H. K. Müller and B. S. Nau, "www.fachwissen-dichtungstechnik.de," 2003. [Online]. Available: www.fachwissen-dichtungstechnik.de/Kapitelseiten/Kapitel17.html. [Accessed 12 January 2023].

[12] A.Berger, T. Polklas, O.Brunn and F. Joos, "Experimental investigation on performance of a control stage turbine under partial admission Paper ID ETC2019-135," Helmut Schmidt University, Hamburg, 2019.